Prisma Sains: Jurnal Pengkajian Ilmu dan Pembelajaran Matematika dan IPA IKIP Mataram
https://e-journal.undikma.ac.id/index.php/prismasains/index
e-mail: prismasains.pkpsm@gmail.com

October 2026. Vol. 14, No. 4
p-ISSN: 2338-4530
e-ISSN: 2540-7899
pp. 2688-2704

Landslide Disaster Mitigation Strategies Using Interpretive Structural Modeling in Talamau District, West Pasaman Regency

[1]*Rizki Amelia Sasqia Putri, [1]Eri Barlian, [1,2]Iswandi Umar, [2]Ratna Wilis, [3]Edward Saleh

[1]Master of Environmental Science Study Program, Universitas Negeri Padang, Padang, Indonesia
[2]Department of Geography, Universitas Negeri Padang, Padang, Indonesia
[3]Agricultural Engineering Study Program, Universitas Sriwijaya, Ogan Ilir, Indonesia

*Corresponding author e-mail: rrizkiasp@student.unp.ac.id

Received: September 2026; Revised: October 2026; Published: October 2026

Abstract

Landslides are a recurring hazard in Talamau District, West Pasaman Regency, affecting communities, settlements, and infrastructure. This study describes recorded landslide occurrences, maps modelled susceptibility for 2015 and 2025, and structures mitigation elements using Interpretive Structural Modeling (ISM). Susceptibility was modelled by integrating slope, rainfall, soil type, geology, and land-use/land-cover (LULC) through a GIS-based weighted overlay. The physical-factor inputs were held constant between the two model runs, while LULC was varied; therefore, the comparison represents changes in modelled susceptibility associated with the LULC input rather than independently verified changes in landslide probability. The area classified as highly susceptible was 14,942.25 ha (36.63%) in 2015 and 16,174.17 ha (39.65%) in 2025. These outputs have not been validated against an independent, spatially referenced landslide inventory. The ISM assessment used eight mitigation elements and a Structural Self-Interaction Matrix agreed upon by three professors during a joint discussion on 3 August 2026. Applying transitive closure to the reachability matrix derived from the reported SSIM yielded E4 as the independent element and E1, E2, E3, E5, E6, E7, and E8 as linkage elements under the stated DPD cut-off. These ISM results describe expert-assessed structural relationships and do not demonstrate the effectiveness of interventions in practice.

Keywords: Landslide; Landslide susceptibility; Disaster mitigation; Interpretive structural modeling; Talamau district.

How to Cite: Putri, R. A. S., Barlian, E., Umar, I., Wilis, R., & Saleh, E. (2026). Landslide Disaster Mitigation Strategies Using Interpretive Structural Modeling in Talamau District, West Pasaman Regency. *Prisma Sains: Jurnal Pengkajian Ilmu Dan Pembelajaran Matematika Dan IPA IKIP Mataram*, *14*(4), 2688–2704. https://doi.org/10.33394/j-ps.v14i4.22699

https://doi.org/10.33394/j-ps.v14i4.22699

Copyright© 2026, Putri et al.
This is an open-access article under the CC-BY License

INTRODUCTION

Landslides are among the natural hazards that frequently occur in Indonesia and affect the environment, infrastructure, and the socioeconomic well-being of communities. The high frequency of landslide occurrences is associated with Indonesia's geographical conditions, which are dominated by hilly and mountainous terrain with relatively high rainfall. Landslide occurrences are influenced by a combination of physical factors, including slope, rainfall, geology, soil type, and land use (Zaenurrohman et al., 2023; Fidan et al., 2024). Differences in these factors result in variations in landslide susceptibility among areas (Gaidzik and Ramírez-Herrera, 2021; Tang et al., 2025). This condition makes landslide susceptibility information important for supporting development planning, land-use management, and disaster risk reduction efforts.

Spatial utilization in sloping areas needs to consider local physical characteristics to reduce the potential for landslides. Land use that is compatible with land capability can help

maintain slope stability. Conversely, uncontrolled land-use change can increase regional vulnerability through vegetation loss and changes in hydrological conditions (Chen et al., 2019; Hao et al., 2022; Xiong et al., 2023; Ballesteros, Martínez-Graña and Yenes, 2024). Vegetation cover also contributes to slope stability through root systems, rainfall interception, and groundwater regulation (Knevels et al., 2021; Zeng et al., 2023). Human activities such as land clearing, construction, and modification of slope conditions can also increase the potential for slope instability (Bozzolan et al., 2022). Therefore, information on landslide susceptibility and land use should be incorporated into decision-making for spatial utilization and sustainable development.

Talamau District is one of the areas in West Pasaman Regency with physical characteristics that may trigger landslides. The district is located within the Bukit Barisan Mountain range and is dominated by hilly to mountainous terrain with relatively steep slopes. High rainfall may also increase soil saturation and trigger mass movement in susceptible areas. These conditions are reflected in the repeated occurrence of landslides in recent years. Based on data from the Badan Penanggulangan Bencana Daerah (BPBD) and Dinas Sosial of West Pasaman Regency, landslide occurrences were recorded in 2019, 2021, 2022, 2023, 2024, and 2025. These occurrences were distributed across several nagari, particularly Nagari Sinuruik, Talu, and Kajai. The recurring pattern indicates that the landslide threat in Talamau District remains ongoing and requires planned mitigation efforts.

The impacts of landslide occurrences in Talamau District also indicate a serious level of threat. In 2019, a landslide affected five people. In 2022, a landslide in Jorong Tabek Sirah, Nagari Talu, caused one fatality and damaged a resident's house. In 2023, a landslide in Polong Anam, Nagari Talu, covered approximately 20 m of road access with landslide material and damaged the electricity network. These conditions disrupted community mobility, economic activities, and daily public services.

Greater impacts occurred in 2024 and 2025. In 2024, landslides in Nagari Sinuruik affected 272 households, displaced 11 households, and damaged 14 houses. In 2025, a landslide in Nagari Sinuruik affected 1,072 households, or approximately 4,727 people, and caused five fatalities. The event also cut off road access in Nagari Sinuruik, while the road in Polong Anam, Nagari Talu, subsided. These damages not only disrupted community mobility but also complicated disaster response operations.

These occurrences indicate that landslides in Talamau District follow a recurring pattern, with varying impacts across periods. This condition highlights the need to understand the temporal dynamics of landslide occurrences and the distribution of areas with different susceptibility levels. Such information is important for identifying areas requiring greater attention and more intensive intervention. Susceptibility mapping can provide a basis for identifying areas with high landslide potential and support spatial planning, infrastructure development, community preparedness, and the prioritization of interventions by local (Silalahi et al., 2019; Guzzetti et al., 2020; Sholichin et al., 2024).

Various studies have used Geographic Information Systems (GIS) to assess landslide susceptibility by integrating slope, rainfall, geology, soil type, and land-use parameters (Sujatha and Sridhar, 2021; Lasaiba, Tetelepta and Ansiska, 2024). These approaches generate spatial information on susceptibility levels that can be used for regional management and disaster risk reduction. Advances in susceptibility modeling have also demonstrated the use of statistical and machine-learning approaches to integrate landslide-controlling factors (Reichenbach et al., 2018; Nhu et al., 2020; Chen and Chen, 2021). Other studies have demonstrated an association between land use and landslide susceptibility because land use is related to surface conditions and human activities in utilizing space (Chen et al., 2019; Moazzam et al., 2020; Zeng et al., 2023; Zhao et al., 2024).

Although landslide susceptibility research has advanced, some studies remain focused on susceptibility mapping and have not integrated information on land-use conditions within

susceptible zones with the formulation of mitigation strategies at the local scale. Each area has distinct physical characteristics, land-use patterns, and susceptibility levels; therefore, mitigation strategies need to be developed according to local conditions. An approach that links landslide susceptibility with land-use conditions can provide a more context-specific basis for regional management (Haryani et al., 2025; Zulfahmi et al., 2025). In Talamau District, information on landslide susceptibility levels, land-use conditions within each susceptibility class, and mitigation strategies appropriate to local characteristics remains limited. This limitation may constrain effective land-use management and disaster risk reduction efforts.

The formulation of mitigation strategies should also consider the interrelationships among the elements involved in landslide risk reduction. Mitigation involves not only physical measures in susceptible areas but also land-use management, community preparedness, institutional strengthening, and coordination in disaster management. These interrelationships need to be understood so that the formulated strategies do not operate in isolation and can be structured according to their degree of interdependence. Interpretive Structural Modeling (ISM) can be used to identify interrelationships among elements, develop a hierarchical structure, and determine elements that play important roles within a system (Umar, Dewata and Barlian, 2019; Ahmad and Qahmash, 2021; Umar and Dewata, 2023).

The unresolved issue in Talamau District is how local landslide records and spatially modelled susceptibility can be translated into a structured set of mitigation priorities while making clear which conclusions come from observed events, GIS model assumptions, and expert judgments. Combining these sources does not, by itself, establish a new modelling method; its local contribution is to organize the available event evidence and susceptibility information alongside expert-assessed relationships among mitigation actions. This study addresses three questions: (1) how have recorded landslide occurrences varied in time, location, and reported impacts; (2) how is modelled susceptibility distributed in 2015 and 2025 when land-use/land-cover is the only input that changes between model runs; and (3) how are the proposed mitigation elements structurally related according to expert judgments? The third question concerns the structure of expert-assessed relationships, not the measured effectiveness of mitigation interventions. The study aims to describe recorded landslide occurrences, map modelled susceptibility, and develop a provisional hierarchy of mitigation elements for Talamau District, West Pasaman Regency. The spatial and ISM outputs must be interpreted within the limits of data completeness, model validation, and the consistency of the underlying matrices.

METHOD

Study Area and Research Period

The study was conducted in Talamau District, West Pasaman Regency, West Sumatra Province (Figure 1). Talamau District was selected because it is characterized by hilly to mountainous terrain, relatively steep slopes, and high rainfall. In addition to its physical characteristics, Talamau District has experienced recurring landslides in recent years, with occurrences distributed across several nagari. The research was conducted in 2026.

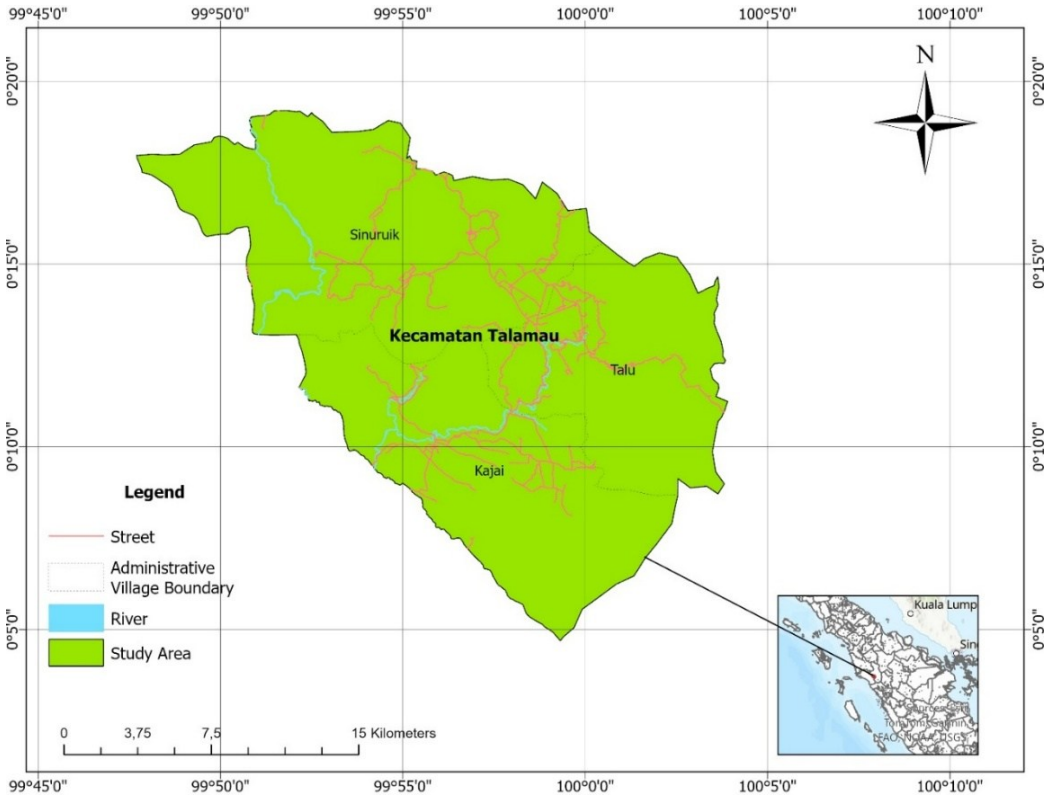


Figure 1. Study Area

Data Types and Sources

The data used in this study are presented in Table 1. The dataset comprises spatial and non-spatial data used to assess landslide susceptibility, analyze land-use/land-cover changes, and develop landslide disaster mitigation strategies in Talamau District, West Pasaman Regency.

Table 1. Data Types and Sources

No.	Data	Data Format	Source
1	Administrative Boundary of Talamau District	Shapefile	RBI Kabupaten Pasaman Barat
2	Elevation Data (DEMNAS)	Raster	Badan Informasi Geospasial (BIG)
3	Slope Data	Raster	Researcher's Analysis
4	Annual Rainfall Data	Excel File	Stasiun Klimatologi Sumatera Barat
5	Geological Data	Shapefile	Dinas PUPR Kabupaten Pasaman Barat
6	Soil Type Data	Shapefile	Dinas PUPR Kabupaten Pasaman Barat
7	Landsat 8 Imagery, 2015	Satellite Imagery	Google Earth Engine
8	Sentinel-2 Imagery, 2025	Satellite Imagery	Google Earth Engine
9	Land-Use Data, 2015	Raster	Researcher's Analysis
10	Land-Use Data, 2025	Raster	Researcher's Analysis
11	Landslide Occurrence Data	Tabular	BPBD, Dinas Sosial Kabupaten Pasaman Barat
12	Field Observation Data	Field Notes and Documentation	Researcher's Survey
13	Community Interview Data	Interview Transcript	Researcher's Interviews
14	Expert Interview Data (Expert Judgment)	Interview Transcript	Researcher's Interviews

All spatial data were processed in ArcGIS Pro and aligned to the study-area extent and common raster geometry before weighted overlay. Slope was derived from DEMNAS using the Slope tool and expressed as percent rise. Annual rainfall values were calculated from available rainfall-station records and interpolated using inverse distance weighting (IDW), after which the rainfall surface was classified into the study's rainfall categories.

The spatial workflow used a cell size of 9.964351 × 9.964351 m (approximately 10 m), with the slope raster as the snap raster. The DEM was projected to WGS 1984 UTM Zone 47N using bilinear resampling while retaining the approximately 10 m cell size. Landsat 8 imagery for 2015 was processed as a median composite with QA_PIXEL cloud masking, while Sentinel-2 imagery for 2025 was processed as a median composite using a Cloud Score Plus threshold of 0.4. Supervised land-cover classification used a Random Forest classifier with 20 trees. The reported overall classification accuracy was 85.60% (Kappa = 0.796) for 2015 and 92.20% (Kappa = 0.795) for 2025. The manuscript does not provide the number and spatial allocation of training and validation samples; this limits independent assessment of classification reliability.

Landslide Occurrence Analysis

Landslide occurrence data were compiled from historical records provided by Badan Penanggulangan Bencana Daerah (BPBD) and Dinas Sosial of West Pasaman Regency. The records covered reported landslide events in Talamau District during the available observation period. The data were organized by event date, location, and reported impacts, including affected households, affected people, and fatalities where such information was available. The compiled records were summarized in tables and graphs and used to produce a spatial distribution map of recorded landslide occurrences.

Temporal analysis grouped the recorded events by year and month to describe the timing of reported occurrences. Locations were examined to provide context for interpreting modelled susceptibility patterns and to identify places where landslides had been documented. The records were compiled from available administrative reports and should not be treated as a complete or independently verified landslide inventory. A dash (–) in Table 2 denotes information unavailable in the source records, not a confirmed zero. Because the records may not capture every event and the available material does not establish a complete deduplication procedure or consistent location accuracy, event frequencies and impacts are interpreted as documented reports rather than a comprehensive account of all landslides in Talamau District.

Landslide Susceptibility Analysis

Landslide susceptibility in Talamau District was modelled using a Geographic Information System (GIS) by integrating five conditioning factors: slope, rainfall, soil type, geology, and land use/land cover (LULC). The analysis was conducted for two temporal snapshots, 2015 and 2025, using the same model structure, factor weights, and class scores. Only the LULC input differed between the two model runs, while slope, rainfall, soil, and geological conditions were held constant. Consequently, the comparison represents changes in modelled susceptibility associated with differences in the LULC input under fixed physical-factor assumptions, rather than a comprehensive assessment of temporal changes in landslide-triggering conditions.

The susceptibility index was calculated using a weighted linear combination:

$$LSI = 0.30S+0.20R+0.15T+0.15G+0.20L$$

where (S) denotes the slope score, (R) the rainfall score, (T) the soil score, (G) the geological score, and (L) the LULC score. Slope was derived from the Indonesian national digital elevation model (DEMNAS) using the Slope tool in ArcGIS Pro and expressed as percent rise. The slope raster was classified into five categories: less than 8%, 8–15%, 15–25%, 25–45%, and greater than 45%, with scores increasing from 1 to 5 as slope steepness increased. Annual rainfall surfaces were generated from rainfall-station records using inverse distance weighting

(IDW). Rainfall was classified into five categories: less than 1,000; 1,000–2,000; 2,000–2,500; 2,500–3,000; and greater than 3,000 mm yr^{-1}, with corresponding scores from 1 to 5. Soil classes were assigned scores according to their relative erosion sensitivity, ranging from 1 for the least sensitive class to 5 for the most sensitive class. Geological units were grouped into alluvial (score 1), volcanic (score 2), sedimentary (score 3), and volcano-sedimentary (score 4). LULC classes were scored as forest or dense vegetation (1), mixed garden or shrubland (2), plantation or paddy field (3), settlement or industrial land (4), and bare land (5). The scoring scheme was adapted from Firdaus and Yuliani (2021) and Fitriyah (2024). The factor weights were assigned as follows: slope 30%, rainfall 20%, soil 15%, geology 15%, and LULC 20%.

Before weighted overlay, the spatial layers were harmonized to a common study-area extent and raster geometry. The raster cell size was approximately 10 m (9.964351 × 9.964351 m), and the slope raster was used as the snap raster. The DEM was projected to WGS 1984 UTM Zone 47N using bilinear resampling while retaining the approximately 10 m cell size. The weighted-overlay index was classified into low, moderate, and high susceptibility using the equal-interval method. The reported index range was 2–5, giving an interval width of 1 and the class intervals 2–less than 3, 3–less than 4, and 4–5. The mapped areas should be interpreted in relation to these model settings and the stated class boundaries.

The resulting maps represent relative, modelled landslide susceptibility based on the selected conditioning factors, class scores, and weights. No independent, spatially referenced landslide inventory was used to validate the susceptibility model; therefore, the mapped classes cannot be interpreted as independently validated probabilities of landslide occurrence. A sensitivity analysis of alternative factor weights was not conducted, so the robustness of the mapped patterns to other plausible weighting schemes remains unknown. Because slope, rainfall, soil type, and geology were held constant between 2015 and 2025, differences between the maps reflect the change in the LULC input under the specified model assumptions. They do not independently demonstrate an increase in actual landslide probability or risk.

Formulation of Mitigation Strategies Using Interpretive Structural Modeling

Mitigation strategies were formulated using Interpretive Structural Modeling (ISM). ISM was used to identify relationships among strategic elements, determine the hierarchical level of each element, and identify elements that play important roles in the landslide disaster mitigation system.

Mitigation strategy elements were identified based on the literature review, landslide occurrence conditions, susceptibility analysis results, and information obtained through interviews with expert informants. Informants were selected purposively based on their knowledge, experience, and involvement in disaster management and landslide-prone areas.

Relationships among strategic elements were analyzed by constructing a Structural Self-Interaction Matrix (SSIM). The SSIM was then converted into a Reachability Matrix to determine the reachability relationships among elements. Level partitioning was subsequently conducted to determine the level of each element. The results were used to construct the hierarchical structure of the mitigation strategy in the form of an ISM model.

The elements in the model were subsequently analyzed based on their driving power and dependence to identify key elements. Elements with strategic roles were used as the basis for determining priorities and directions for landslide disaster mitigation in Talamau District. The final ISM results were then interpreted by considering landslide occurrence conditions, temporal dynamics, and regional susceptibility.

RESULT AND DISCUSSION

Characteristics and Distribution of Landslide Occurrences

Talamau District has experienced recurring landslide occurrences in recent years. Based on landslide occurrence data obtained from the BPBD and Social Affairs Office of West Pasaman Regency, landslides were recorded in 2019, 2021, 2022, 2023, 2024, and 2025. These

occurrences were distributed across several areas of Talamau District, particularly Nagari Sinuruik, Nagari Talu, and Nagari Kajai. This distribution indicates that landslides are not concentrated in a single location but occur across several parts of the district with different environmental characteristics (Table 2).

Table 2. Summary of Landslide Disaster Occurrences in West Pasaman Regency, 2019–2025

Date of Occurrence	Location	Affected Households	Affected People	Deaths	Other Impacts
16 January 2019	Talamau District	–	5	–	Road subsidence
13 August 2021	Nagari Sinuruik, Talamau District	–	–	–	Road subsidence
10 November 2021	Nagari Sinuruik, Talamau District	–	–	–	Road subsidence
21 June 2022	Jorong Tabek Sirah, Nagari Talu, Talamau District	1	1	1	Road subsidence
16 November 2022	Jorong Kampung Alang, Nagari Kajai, Talamau District	1	1	–	Road subsidence
1 December 2022	Jorong Kampung Alang, Nagari Kajai, Talamau District	1	–	–	Road subsidence
19 August 2023	Polong Anam, Nagari Talu, Talamau District	–	–	–	Road subsidence
19 October 2023	Polong Anam, Nagari Talu, Talamau District	–	–	–	Landslide material covered approximately 20 m of road and damaged the electricity network
3 March 2024	Nagari Sinuruik, Talamau District	–	–	–	Road access cut off
7 March 2024	Jorong Limpato, Nagari Kajai, Talamau District	–	–	–	Road access cut off
3 April 2024	Nagari Sinuruik, Talamau District	272	–	–	11 households evacuated; 14 houses damaged
24 November 2025	Nagari Sinuruik, Talamau District	1,072	4,727	5	Road access cut off
19 December 2025	Polong Anam, Nagari Talu, Talamau District	–	–	–	Road subsidence

Note: A dash (–) indicates that the relevant impact information was unavailable in the source records; it does not mean that the value was zero.

Table 2 presents the characteristics of landslide occurrences in terms of timing, location, and impacts. The variation in impacts among events indicates that landslides have different levels of consequences for communities and infrastructure. Some events directly affected communities, whereas others disrupted transportation access and infrastructure networks.

Historically, the 2019 event affected five people. In 2022, a landslide in Jorong Tabek Sirah, Nagari Talu, caused one fatality and damaged a resident's house. In 2023, a landslide in

Polong Anam, Nagari Talu, covered approximately 20 m of road access with landslide material and damaged the electricity network. These conditions show that landslide impacts are not limited to land damage but can also disrupt accessibility and public services.

The impacts increased in 2024 and 2025. In 2024, landslides in Nagari Sinuruik affected 272 households, displaced 11 households, and damaged 14 houses. In 2025, a landslide in Nagari Sinuruik affected 1,072 households, or approximately 4,727 people, and caused five fatalities. The event also cut off road access in Nagari Sinuruik, while the road in Polong Anam, Nagari Talu, subsided.

Land-Use/Land-Cover Change in Talamau District, 2015–2025

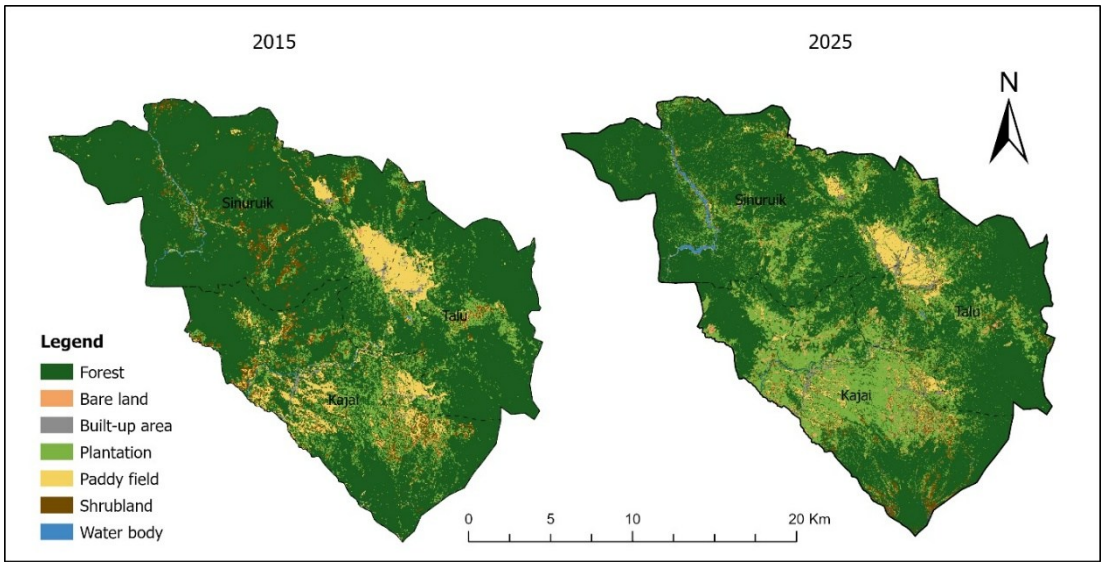


Figure 2. Spatial Distribution of Land Use and Land Cover in Talamau District in 2015 and 2025

Table 3. Land-Use/Land-Cover Area and Change in Talamau District, 2015–2025

No	Land-Use Category	2015 (ha)	2025 (ha)	Change (ha)	Change (%)
1	Forest	31,008.57	26,713.75	-4,294.81	-13.85%
2	Bare Land	126.40	514.07	+387.66	+306.68%
3	Built-Up Area	230.21	271.20	+40.99	+17.80%
4	Plantation	4,446.91	9,580.40	+5,133.48	+115.44%
5	Paddy Field	2,816.49	1,725.45	-1,091.04	-38.74%
6	Shrubland	2,029.58	1,734.97	-294.61	-14.52%
7	Water Bodies	134.20	252.53	+118.33	+88.18%
	Total	40,792.37	40,792.37		

The land-use/land-cover maps show changes in the distribution and area of the seven mapped classes in Talamau District between 2015 and 2025. As summarized in Table 3, forest remained the largest class in both years, but its mapped area decreased from 31,008.57 ha in 2015 to 26,713.75 ha in 2025, a net reduction of 4,294.81 ha (13.85% relative to the 2015 area). Over the same period, plantation area increased from 4,446.91 ha to 9,580.40 ha, a net gain of 5,133.48 ha (115.44%).

Other classes also changed. Paddy-field area decreased by 1,091.04 ha (38.74%), while shrubland decreased by 294.61 ha (14.52%). In contrast, mapped bare land increased by 387.66 ha (306.68%), built-up land increased by 40.99 ha (17.80%), and water bodies increased by 118.33 ha (88.18%). These values describe net differences in mapped class areas between the two dates; they do not, by themselves, identify the exact locations or pathways of transitions from one land-cover class to another.

The most prominent net changes were the reduction in forest area and the expansion of plantations. These patterns are relevant to landslide mitigation because vegetation cover and

land management are among the factors considered in the susceptibility model and in the proposed mitigation elements. However, the classified maps alone do not establish that the observed land-cover changes caused landslides or increased actual landslide probability. In this study, land-use/land-cover was the only input varied between the 2015 and 2025 susceptibility model runs, while slope, rainfall, soil type, and geology were held constant.

The comparison of total class areas should therefore be interpreted as a summary of net land-cover change. A full land-use transition matrix, calculated by overlaying the 2015 and 2025 classified rasters, would be needed to quantify specific transitions (for example, forest to plantation or shrubland to bare land). Such transition pathways cannot be reconstructed reliably from the aggregate area totals in Table 3 alone.

Landslide Susceptibility in 2015 and 2025

Landslide susceptibility was modelled for 2015 and 2025 by integrating slope, rainfall, soil type, geology, and LULC. The same physical-factor layers, factor weights, and class scores were used for both years; only the LULC layer differed. The comparison therefore isolates the effect of the LULC input within the selected model framework and should not be interpreted as a comprehensive assessment of temporal changes in landslide-triggering conditions (Figure 3).

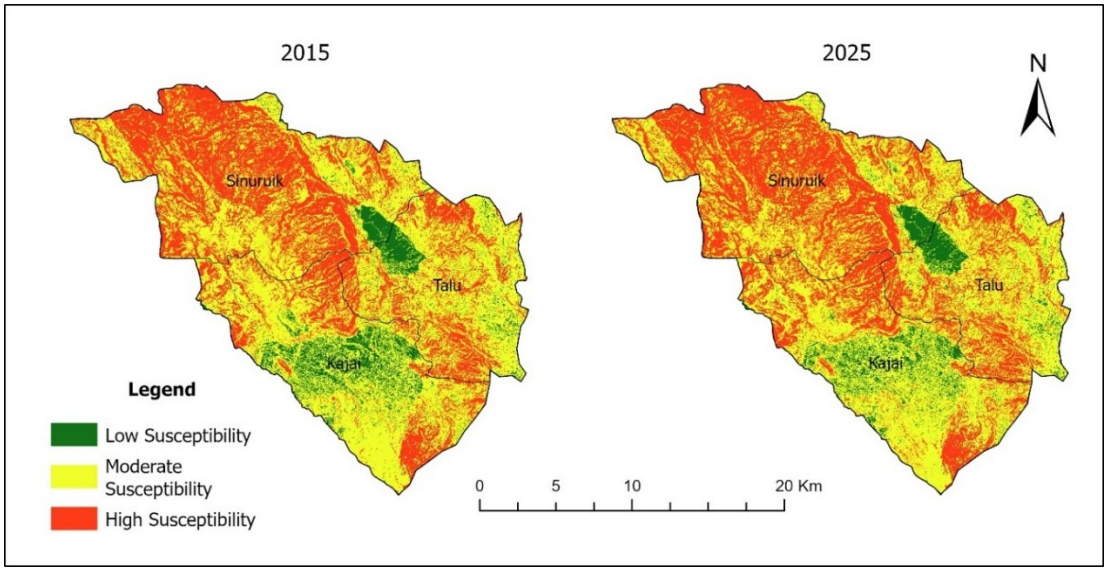


Figure 3. Landslide Susceptibility Map of Talamau District in 2015 and 2025

The results show that the moderate susceptibility class dominated Talamau District in both 2015 and 2025. In 2015, the moderate susceptibility class covered 22,509.23 ha, or 55.18% of the study area. In 2025, the area of the moderate susceptibility class decreased to 21,754.57 ha, or 53.33%. Meanwhile, the high susceptibility class increased from 14,942.25 ha, or 36.63%, in 2015 to 16,174.17 ha, or 39.65%, in 2025 (Table 4).

Table 4. Area and Percentage of Landslide Susceptibility Classes in Talamau District in 2015 and 2025

Susceptibility Class	2015 (ha)	2015 (%)	2025 (ha)	2025 (%)
Low Susceptibility	3.340,90	8,19	2.863,62	7,02
Moderate Susceptibility	22.509,23	55,18	21.754,57	53,33
High Susceptibility	14.942,25	36,63	16.174,17	39,65
Total	40.792,37	100,00	40.792,37	100,00

Comparison of the two years shows that the low susceptibility class decreased by 477.28 ha, from 3,340.90 ha in 2015 to 2,863.62 ha in 2025. The moderate susceptibility class also decreased by 754.66 ha, from 22,509.23 ha to 21,754.57 ha. Conversely, the high susceptibility class increased by 1,231.92 ha, from 14,942.25 ha to 16,174.17 ha.

The differences between the two maps are associated with the LULC inputs used in the 2015 and 2025 model runs, while slope, rainfall, soil type, and geology were held constant. The mapped shift therefore describes how the specified weighted-overlay model responds to differences in LULC scores. It does not establish that physical landslide hazard or actual landslide probability increased over the period.

The area classified as highly susceptible increased by 1,231.92 ha, equivalent to 3.02 percentage points of the study area. The low and moderate classes decreased by 477.28 ha and 754.66 ha, respectively. These are differences in class areas between two model outputs; without a cell-by-cell susceptibility transition matrix and independent validation, the figures should not be interpreted as the measured movement of specific locations between susceptibility classes or as proof of increased landslide probability.

The susceptibility maps, recorded landslide reports, and field observations were considered together when identifying the local context for the proposed mitigation elements. However, because the event records were not used as an independent validation inventory and the manuscript does not quantify the spatial overlap between event locations and susceptibility classes, this integration is interpretive rather than a statistical validation of the maps.

Field Observations of Landslide Remnants

Field observations were conducted to identify physical conditions, particularly at locations showing indications of past or recent landslide activity. The observations revealed variations in slope conditions, vegetation cover, slope exposure, and the presence of roads in sloping areas. Several locations showed indications of past landslides, characterized by changes in slope morphology, accumulated soil material, unstable ground surfaces, and exposed vegetation cover (Figure 4).

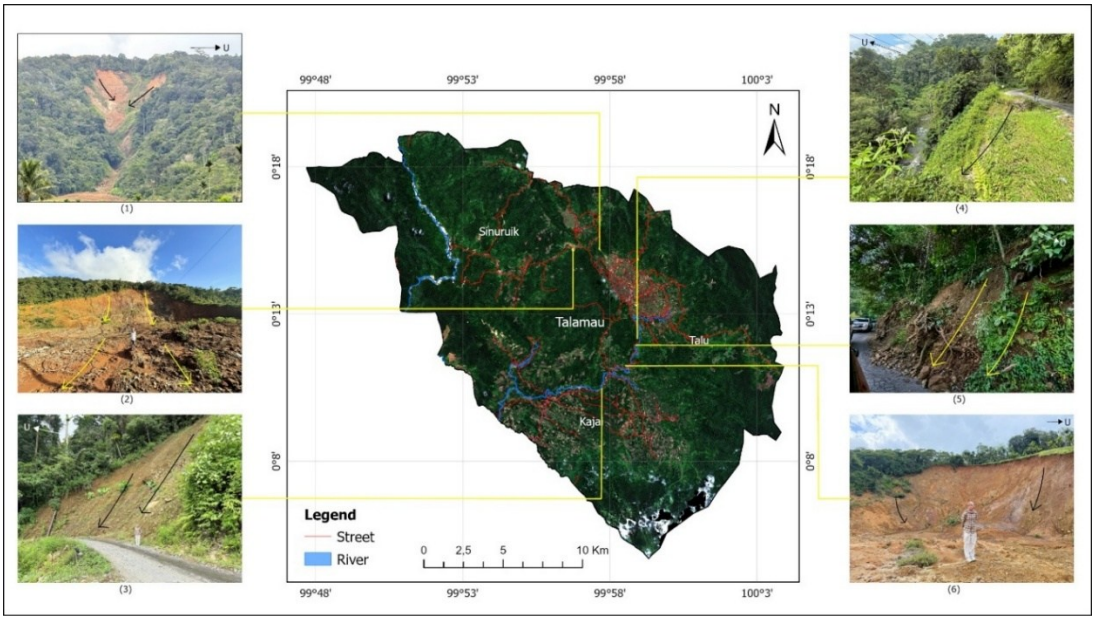


Figure 4. Field Observations of Landslide Remnants in the Study Area

Table 5. Field Observation Locations and Corresponding Landslide Susceptibility Classes

Field observation	Coordinate	Location	Susceptibility class
Site 1	0.243320 99.970204	Sinuruik	High
Site 2	0.254303 99.946170	Sinuruik	High
Site 3	0.174664 99.962253	Kajai	High
Site 4	0.203018	Talu	High

Field observation	Coordinate	Location	Susceptibility class
Sita 5	99.982393 0.199295	Talu	High
Site 6	99.981529 0.254303	Talu	High
	99.946170		

The field documentation shows slopes with altered morphology and signs of instability, both on exposed slopes and on slopes adjacent to roads. Several locations also showed displaced soil and rock material and slope sections exposed as a result of landsliding.

The field documentation shows slopes with altered morphology and signs of instability, including exposed slopes and slopes adjacent to roads, as well as displaced soil or rock material. These observations provide qualitative context for the study area. The photographs are not, by themselves, a dated or georeferenced landslide inventory, and the available manuscript does not provide coordinates and observation dates for each photographed site. Accordingly, the images are used as field context rather than as independent validation of the susceptibility model.

Formulation of Landslide Disaster Mitigation Strategies Using ISM

Landslide disaster mitigation strategies were formulated using Interpretive Structural Modeling (ISM) to identify relationships among strategic elements, determine the position of each element based on its driving power and dependence, and construct the hierarchical structure of mitigation strategies. The ISM analysis comprised the identification of strategic elements, assessment of inter-element relationships using VAXO, Driver Power–Dependence (DPD) analysis, and hierarchical level structuring.

Identification of Strategic Elements

Strategic elements were identified based on expert interviews, a literature review, landslide susceptibility analysis, field observations, and a review of relevant policy documents. This process resulted in eight strategic elements used in the ISM analysis (Table 6).

Table 6. Landslide Disaster Mitigation Strategy Elements

Code	Strategic Element	Aspect
E1	Control of land-use change in landslide-susceptible areas.	Land-Use Management
E2	Rehabilitation of degraded land and enhancement of vegetation cover in landslide-susceptible areas.	Environmental Conservation
E3	Application of soil and water conservation techniques on sloping land.	Environmental Conservation
E4	Strengthening policies and monitoring of spatial utilization and land-use conversion.	Policy and Monitoring
E5	Use of landslide susceptibility information in development planning and regional management.	Spatial Planning
E6	Enhancement of community capacity and participation in land management and landslide mitigation.	Community Empowerment
E7	Strengthening coordination among stakeholders in landslide disaster mitigation.	Institutional Capacity
E8	Strengthening landslide monitoring, preparedness, and early warning systems.	Disaster Preparedness

These eight elements were subsequently used to identify contextual relationships among elements through expert assessment using the VAXO approach.

VAXO Assessment and Value Conversion

Inter-element relationships were assessed using the symbols V, A, X, and O. V indicates that the row element influences the column element; A indicates that the column element influences the row element; X indicates a reciprocal relationship; and O indicates no direct

contextual relationship. Three professors from Universitas Negeri Padang (UNP) were purposively selected because of their academic expertise in environmental science, environmental geography, geography, and disaster-related studies, including scholarly work on disaster issues. On 3 August 2026, the three experts jointly discussed and assessed the contextual relationships among the proposed mitigation elements. The agreed judgments were recorded in the Structural Self-Interaction Matrix (SSIM) shown in Table 7. As the experts assessed the matrix jointly, the SSIM represents the outcome of their discussion rather than a numerical aggregation of three independent matrices.

Table 7. Structural Self-Interaction Matrix

	Element	j							
		E1	E2	E3	E4	E5	E6	E7	E8
i	E1		X	X	A	V	X	V	X
	E2			X	A	V	X	V	X
	E3				A	X	V	V	X
	E4					V	V	V	V
	E5						A	A	X
	E6							V	V
	E7								V
	E8								

The SSIM records the experts' agreed VAXO judgments and was retained unchanged. It was converted into an initial reachability matrix using the standard rules: V assigns 1 to the row-to-column direction and 0 to the reverse direction; A assigns 0 to the row-to-column direction and 1 to the reverse direction; X assigns 1 in both directions; and O assigns 0 in both directions. Diagonal entries were set to 1. The initial matrix was then subjected to transitive closure. This procedure adds implied indirect reachability links to the derived matrix; it does not change the original VAXO judgments in the SSIM.

Table 8. Initial Reachability Matrix

	Element	**j**								**DP**
		E1	**E2**	**E3**	**E4**	**E5**	**E6**	**E7**	**E8**	
i	E1	1	1	1	0	1	1	1	1	7
	E2	1	1	1	0	1	1	1	1	7
	E3	1	1	1	0	1	1	1	1	7
	E4	1	1	1	1	1	1	1	1	8
	E5	0	0	1	0	1	0	0	1	3
	E6	1	1	0	0	1	1	1	1	6
	E7	0	0	0	0	1	0	1	1	3
	E8	1	1	1	0	1	0	0	1	5
	D	6	6	6	1	8	5	6	8	

Note: DP = driving power. This initial matrix was obtained by converting the SSIM using the VAXO rules.

The SSIM-to-reachability conversion produced the initial binary matrix in Table 8. The diagonal entries were set to 1, and the remaining entries were assigned according to the VAXO conversion rules. The initial matrix represents the direct relationships encoded by the experts' agreed SSIM; indirect relationships implied by paths through other elements are added in the final reachability matrix through transitive closure.

Table 9. Final Reachability Matrix after Transitive Closure

Element	**E1**	**E2**	**E3**	**E4**	**E5**	**E6**	**E7**	**E8**	**DP**
E1	1	1	1	0	1	1	1	1	7
E2	1	1	1	0	1	1	1	1	7
E3	1	1	1	0	1	1	1	1	7
E4	1	1	1	1	1	1	1	1	8

Element	E1	E2	E3	E4	E5	E6	E7	E8	DP
E5	1	1	1	0	1	1	1	1	7
E6	1	1	1	0	1	1	1	1	7
E7	1	1	1	0	1	1	1	1	7
E8	1	1	1	0	1	1	1	1	7
Dependence	8	8	8	1	8	8	8	8	

Note: DP = driving power. The final reachability matrix was obtained by applying transitive closure to the initial reachability matrix.

Transitive closure added the indirect relationships required for consistency. For example, the SSIM-derived initial matrix indicated E5 → E3 and E3 → E1; therefore, the final matrix also includes E5 → E1. Similarly, because E8 → E1 and E1 → E6, the final matrix includes E8 → E6. The same rule was applied to all implied paths. Based on the resulting final reachability matrix, E4 has a driving power of 8 and dependence of 1. Each of E1, E2, E3, E5, E6, E7, and E8 has a driving power of 7 and dependence of 8. These values are derived from the SSIM presented in Table 7 and should be understood as the structural consequences of the experts' agreed judgments.

Driver Power–Dependence Matrix

The driver power and dependence values obtained from the Final Reachability Matrix were used to map the position of each element in the DPD matrix. Driver power represents an element's ability to influence other elements, whereas dependence represents the extent to which an element depends on other elements (Figure 5).

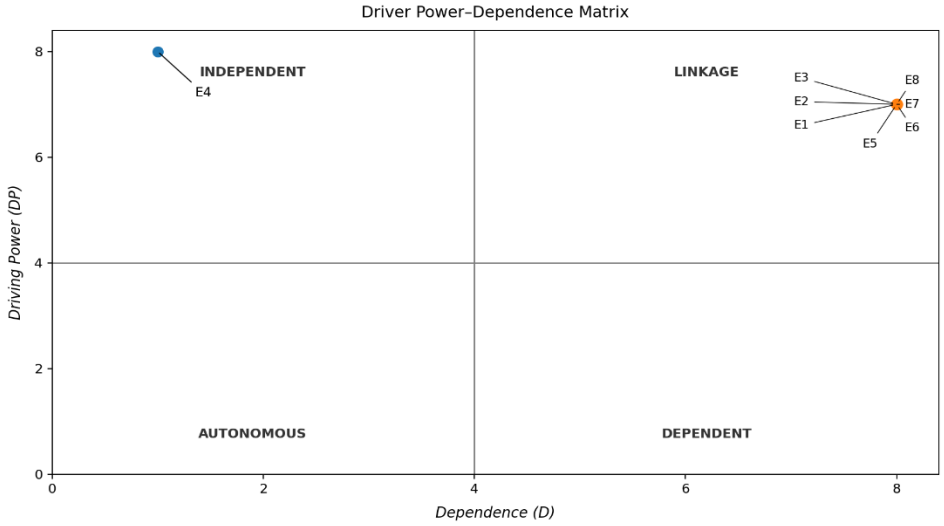


Figure 5. Driver Power–Dependence Matrix

Using the final reachability matrix, E4 has driving power 8 and dependence 1, whereas E1, E2, E3, E5, E6, E7, and E8 each have driving power 7 and dependence 8. Using 4 as the cut-off value on both axes, E4 falls in the Independent quadrant, while the other seven elements fall in the Linkage quadrant. No element falls in the Autonomous or Dependent quadrants. The concentration of seven elements in the Linkage quadrant indicates that, under the reported SSIM, these elements are mutually connected through direct and/or indirect reachability and should not be interpreted as an independent ranking of intervention effectiveness.

The DPD classification is based on the final reachability matrix and a cut-off value of 4 for both driving power and dependence. This threshold is the midpoint of the 0–8 scale displayed in Figure 5. The quadrant positions describe the structural pattern generated by the SSIM; they do not measure the real-world effectiveness, feasibility, or urgency of each intervention.

ISM Hierarchical Levels

Hierarchical levels were determined from the final reachability matrix using the reachability set, antecedent set, and intersection set. Under the matrix derived from the SSIM in Table 7, E1, E2, E3, E5, E6, E7, and E8 form Level I, while E4 forms Level II (Table 10 and Figure 6). This partition reflects the reachability structure of the reported matrix. Because the seven Level I elements are mutually reachable in the transitive closure, their placement at the same level does not establish an order of priority among them.

Table 10. Hierarchical Levels of Mitigation Strategy Elements

No.	Level I	Level II
1	E1	E4
2	E2	
3	E3	
4	E5	
5	E6	
6	E7	
7	E8	

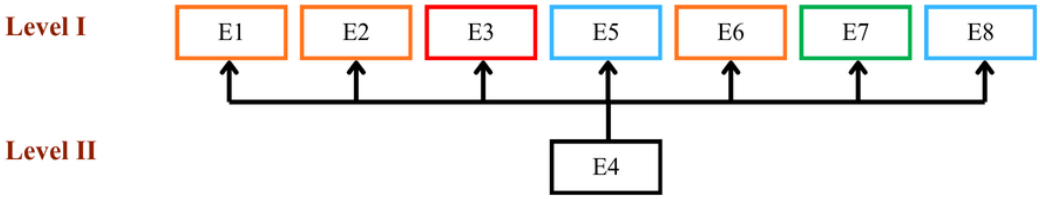


Figure 6. Interpretive Structural Modeling Hierarchy

The hierarchy places E4 at Level II as the underlying driver in the reachability structure, with E1, E2, E3, E5, E6, E7, and E8 at Level I. In practical terms, the experts' judgments position policy and spatial-use monitoring as a structural driver connected to land-use control, land rehabilitation, soil and water conservation, planning, community participation, institutional coordination, and preparedness. This structure reflects expert-assessed relationships; it does not demonstrate that E4 is the most effective or most urgent intervention in practice.

CONCLUSIONS

Available administrative records document landslide occurrences in Talamau District in 2019, 2021, 2022, 2023, 2024, and 2025, particularly in Nagari Sinuruik, Nagari Talu, and Nagari Kajai. The largest reported impacts in the compiled dataset occurred in 2025. However, several impact fields were unavailable, and the available information does not establish that the records form a complete, independently verified, and fully deduplicated inventory. The findings therefore describe recorded events and should not be used alone to infer temporal changes in landslide probability.

The weighted-overlay model classified the largest share of Talamau District as moderately susceptible in both years. The area classified as highly susceptible was 14,942.25 ha (36.63%) in 2015 and 16,174.17 ha (39.65%) in 2025, a difference of 1,231.92 ha or 3.02 percentage points. Because slope, rainfall, soil type, and geology were held constant and only LULC was changed, this difference represents the response of the model to the LULC input under fixed assumptions. It is not independent evidence of an increase in actual landslide probability or risk. The maps were not validated using an independent spatial landslide inventory, and sensitivity to alternative factor weights was not tested.

The study identified eight proposed mitigation elements and examined their structural relationships using an SSIM agreed upon by three professors during a joint discussion on 3 August 2026. Transitive closure of the SSIM-derived initial reachability matrix gives E4 a driving power of 8 and dependence of 1; E1, E2, E3, E5, E6, E7, and E8 each have driving power 7 and dependence 8. With a cut-off of 4 on both DPD axes, E4 is classified as

Independent and the other seven elements as Linkage. The hierarchy places E4 at Level II and the remaining elements at Level I. These results represent expert-assessed structural relationships, not measured intervention effectiveness. Overall, the findings provide a local descriptive basis for considering landslide reports, modelled susceptibility, and mitigation planning, subject to limitations in inventory completeness, spatial validation, and the scope of the weighted-overlay comparison.

ACKNOWLEDGMENTS

The authors gratefully acknowledge Universitas Negeri Padang for institutional support, the Regional Disaster Management Agency (BPBD) and Social Affairs Office of West Pasaman Regency for providing landslide disaster data, and the experts and local communities who contributed valuable information and insights during the research.

FUNDING INFORMATION

This research received no external funding and was entirely self-funded by the first author.

AUTHOR CONTRIBUTIONS STATEMENT

Name of Author	C	M	So	Va	Fo	I	R	D	O	E	Vi	Su	P	Fu
Rizki Amelia Sasqia Putri	✓	✓	✓		✓	✓	✓	✓	✓	✓	✓		✓	✓
Eri Barlian	✓	✓		✓						✓		✓		
Iswandi Umar		✓		✓						✓		✓		
Ratna Wilis				✓						✓		✓		
Edward Saleh										✓				

CONFLICT OF INTEREST STATEMENT

The authors declare that they have no known competing financial interests or personal relationships that could have appeared to influence the work reported in this paper.

ETHICAL APPROVAL

The study was conducted with institutional research permission from Universitas Negeri Padang. Participation in community interviews and expert assessments was voluntary, and participants were informed of the research objectives before providing information. All collected information was used exclusively for academic research purposes.

DATA AVAILABILITY

The study utilized administrative landslide records, spatial datasets, and expert assessment data. The processed spatial outputs and Interpretive Structural Modeling (ISM) matrices are available from the corresponding author upon reasonable request, subject to applicable data-sharing permissions. Third-party datasets remain subject to the access policies of their respective providers.

REFERENCES

Ahmad, N., & Qahmash, A. (2021). SmartISM: Implementation and assessment of interpretive structural modeling. *Sustainability, 13*(16), Article 8801. https://doi.org/10.3390/su13168801

Alam, E., & Ray-Bennett, N. S. (2021). Disaster risk governance for district-level landslide risk management in Bangladesh. *International Journal of Disaster Risk Reduction, 59*, Article 102220. https://doi.org/10.1016/j.ijdrr.2021.102220

Bozzolan, E., Holcombe, E. A., Pianosi, F., Marchesini, I., Alvioli, M., & Wagener, T. (2023). A mechanistic approach to include climate change and unplanned urban sprawl in landslide susceptibility maps. *Science of the Total Environment, 858*, Article 159412. https://doi.org/10.1016/j.scitotenv.2022.159412

Buenahora Ballesteros, C. A., Martínez-Graña, A. M., & Yenes, M. (2024). Influence of cumulative geotechnical deterioration on mass movement at a medium-scale regional analysis (Cortinas Sector, Toledo, Colombia). *Land, 13*(7), Article 1000. https://doi.org/10.3390/land13071000

Chen, L., Guo, Z., Yin, K., Shrestha, D. P., & Jin, S. (2019). The influence of land use and land cover change on landslide susceptibility: A case study in Zhushan Town, Xuan'en County (Hubei, China). *Natural Hazards and Earth System Sciences, 19*(10), 2207–2228. https://doi.org/10.5194/nhess-19-2207-2019

Chen, X., & Chen, W. (2021). GIS-based landslide susceptibility assessment using optimized hybrid machine learning methods. *Catena, 196*, Article 104833. https://doi.org/10.1016/j.catena.2020.104833

Dieng, M., Mbow, C., Skole, D. L., & Ba, B. (2023). Sustainable land management policy to address land degradation: Linking old forest management practices in Senegal with new REDD+ requirements. *Frontiers in Environmental Science, 11*, Article 1088726. https://doi.org/10.3389/fenvs.2023.1088726

Fidan, S., Tanyaş, H., Akbaş, A., Lombardo, L., Petley, D. N., & Görüm, T. (2024). Understanding fatal landslides at global scales: A summary of topographic, climatic, and anthropogenic perspectives. *Natural Hazards, 120*(7), 6437–6455. https://doi.org/10.1007/s11069-024-06487-3

Gaidzik, K., & Ramírez-Herrera, M. T. (2021). The importance of input data on landslide susceptibility mapping. *Scientific Reports, 11*, Article 19334. https://doi.org/10.1038/s41598-021-98830-y

Guzzetti, F., Gariano, S. L., Peruccacci, S., Brunetti, M. T., Marchesini, I., Rossi, M., & Melillo, M. (2020). Geographical landslide early warning systems. *Earth-Science Reviews, 200*, Article 102973. https://doi.org/10.1016/j.earscirev.2019.102973

Hao, L., van Westen, C., Rajaneesh, A., Sajinkumar, K. S., Martha, T. R., & Jaiswal, P. (2022). Evaluating the relation between land use changes and the 2018 landslide disaster in Kerala, India. *Catena, 216*, Article 106363. https://doi.org/10.1016/j.catena.2022.106363

Haryani, Barlian, E., Tela, I. N., Aditia, E., & Putra, A. (2025). GIS-based analysis of slope, landslide and flood hazards, and land use integrated with indigenous knowledge in Nagari Sijunjung, Indonesia. *Geographia Technica, 20*(2), 336–353. https://doi.org/10.21163/GT_2025.202.21

Knevels, R., Brenning, A., Gingrich, S., Heiss, G., Lechner, T., Leopold, P., Plutzar, C., Proske, H., & Petschko, H. (2021). Towards the use of land use legacies in landslide modeling: Current challenges and future perspectives in an Austrian case study. *Land, 10*(9), Article 954. https://doi.org/10.3390/land10090954

Lasaiba, M. A., Tetelepta, E. G., & Ansiska, P. (2024). Assessment of landslide vulnerability in urban areas using GIS and remote sensing: A study in Ambon City. *Jurnal Geografi, 16*(1), 32–50. https://doi.org/10.24114/jg.v16i1.41978

Moazzam, M. F. U., Vansarochana, A., Boonyanuphap, J., Rahman, G., Djueyep, G. P., & Choosumrong, S. (2020). Spatio-statistical comparative approaches for landslide susceptibility modeling: Case of Mae Phun, Uttaradit Province, Thailand. *SN Applied Sciences, 2*, Article 384. https://doi.org/10.1007/s42452-020-2106-8

Nepal, P., Khanal, N. R., Zhang, Y., Paudel, B., & Liu, L. (2020). Land use policies in Nepal: An overview. *Land Degradation & Development, 31*(16), 2203–2212. https://doi.org/10.1002/ldr.3621

Nhu, V.-H., Mohammadi, A., Shahabi, H., Ahmad, B. B., Al-Ansari, N., Shirzadi, A., Geertsema, M., Kress, V. R., Karimzadeh, S., Valizadeh Kamran, K., Chen, W., & Nguyen, H. (2020). Landslide detection and susceptibility modeling on Cameron Highlands (Malaysia): A comparison between random forest, logistic regression and logistic model tree algorithms. *Forests, 11*(8), Article 830. https://doi.org/10.3390/f11080830

Reichenbach, P., Rossi, M., Malamud, B. D., Mihir, M., & Guzzetti, F. (2018). A review of statistically-based landslide susceptibility models. *Earth-Science Reviews, 180*, 60–91. https://doi.org/10.1016/j.earscirev.2018.03.001

Sholichin, M., Othman, F., Prayogo, T. B., & Rahardjo, S. S. P. (2024). Assessing landslide susceptibility and formulating adaptation strategies in the Konto Watershed, East Java, Indonesia. *International Journal of Disaster Risk Reduction, 113*, Article 104797.

https://doi.org/10.1016/j.ijdrr.2024.104797

Silalahi, F. E. S., Pamela, Arifianti, Y., & Hidayat, F. (2019). Landslide susceptibility assessment using frequency ratio model in Bogor, West Java, Indonesia. *Geoscience Letters, 6*, Article 10. https://doi.org/10.1186/s40562-019-0140-4

Situmorang, R. O. P., Wijaya, N., Hafsari, T. A., Putra Pasaribu, P. H., & Anggraeni, R. (2025). Governance of housing spatial planning of Semarang City in landslide mitigation and the influence of biophysical, climatic, and socio-economic factors. *Planning Malaysia, 23*(38), 128–143. https://doi.org/10.21837/pm.v23i38.1783

Sujatha, E. R., & Sridhar, V. (2021). Landslide susceptibility analysis: A logistic regression model case study in Coonoor, India. *Hydrology, 8*(1), Article 41. https://doi.org/10.3390/hydrology8010041

Tang, Z., Zheng, X., Pan, J., Huang, X., Zhu, L., Wang, N., Xie, M., Yan, G., Wang, C., Wang, Z., Xu, C., & Song, C. (2025). Spatial joint hazard assessment of landslide susceptibility and intensity within a single framework: Environmental insights from the Wenchuan earthquake. *Science of the Total Environment, 963*, Article 178545. https://doi.org/10.1016/j.scitotenv.2025.178545

Tayebi, S., Jabed, M. A., Ruano, A. L., Lee, G. O., da Silva, P. F., Ahmed, S., Aristizábal G., E. V., Dahal, R. K., Soltani, A., Khan, M. I., Rahman, M. A., Islam, M. A., & Haque, U. (2024). Stakeholder perspectives on landslide triggers and impacts in five countries. *Landslides, 21*(8), 2033–2043. https://doi.org/10.1007/s10346-024-02270-4

Umar, I., & Dewata, I. (2023). *Pendekatan sistem dalam manajemen sumber daya alam*. Deepublish.

Umar, I., Dewata, I., & Barlian, E. (2019). Dynamic model of land use change in landslide hazard zones in Tanah Datar District, West Sumatra. *IOP Conference Series: Earth and Environmental Science, 314*(1), Article 012070. https://doi.org/10.1088/1755-1315/314/1/012070

Xiong, H., Ma, C., Li, M., Tan, J., & Wang, Y. (2023). Landslide susceptibility prediction considering land use change and human activity: A case study under rapid urban expansion and afforestation in China. *Science of the Total Environment, 866*, Article 161430. https://doi.org/10.1016/j.scitotenv.2023.161430

Zaenurrohman, J. A., Permanajati, I., Nuraga, P. B., & Setijadi, R. (2023). Kerentanan gerakan tanah menggunakan analisis data spasial di daerah Karangjambu, Purbalingga. *GEOGRAPHY: Jurnal Kajian, Penelitian dan Pengembangan Pendidikan, 11*(1), 158–171. https://doi.org/10.31764/geography.v11i1.14380

Zeng, T., Guo, Z., Wang, L., Jin, B., Wu, F., & Guo, R. (2023). Tempo-spatial landslide susceptibility assessment from the perspective of human engineering activity. *Remote Sensing, 15*(16), Article 4111. https://doi.org/10.3390/rs15164111

Zhao, F., Miao, F., Wu, Y., Gong, S., Zheng, G., Yang, J., & Zhan, W. (2024). Landslide dynamic susceptibility mapping in urban expansion area considering spatiotemporal land use and land cover change. *Science of the Total Environment, 949*, Article 175059. https://doi.org/10.1016/j.scitotenv.2024.175059

Zulfahmi, Z., Putra, M. H. Z., Sarah, D., Tohari, A., Madiutomo, N., Hartanto, P., & Damayanti, R. (2025). GIS-based landslide susceptibility mapping with a blended ensemble model and key influencing factors in Sentani, Papua, Indonesia. *Geosciences, 15*(10), Article 390. https://doi.org/10.3390/geosciences15100390